Signatures of Quantum Stability in a Classically Chaotic System

S. Schlunk,[1] M. B. d'Arcy,[1] S. A. Gardiner,[1] D. Cassettari,[1] R. M. Godun,[1] and G. S. Summy[1,2]

[1]*Clarendon Laboratory, Department of Physics, University of Oxford, Parks Road, Oxford, OX1 3PU, United Kingdom*

[2]*Department of Physics, Oklahoma State University, Stillwater, Oklahoma 74078-3072*

(Received 20 June 2002; published 3 February 2003)

We experimentally and numerically investigate the quantum accelerator mode dynamics of an atom optical realization of the quantum δ-kicked accelerator, whose classical dynamics are chaotic. Using a Ramsey-type experiment, we observe interference, demonstrating that quantum accelerator modes are formed coherently. We construct a link between the behavior of the evolution's fidelity and the phase space structure of a recently proposed pseudoclassical map, and thus account for the observed interference visibilities.

DOI: 10.1103/PhysRevLett.90.054101 PACS numbers: 05.45.Mt, 03.65.Sq, 32.80.Lg, 42.50.Vk

The way in which macroscopic classical phenomena originate in the quantum regime remains a subject of dispute [1]. The issues involved are particularly marked for quantum versions of classically chaotic systems [2]. Experimental investigations of such systems began with studies of microwave-driven hydrogen [3]; subsequent work has also centered on microwave cavities [4], mesoscopic solid-state systems [5], and atom optics [6], the approach we adopt. In this Letter we consider the quantum δ-kicked accelerator [7–9], a δ-kicked rotor with an additional static linear potential. The δ-kicked rotor is one of the most extensively investigated systems in chaotic dynamics [10], and is equivalent to a free particle subjected periodically to instantaneous momentum kicks from a sinusoidal potential. Quantum mechanically, the effect of these kicks is to diffract the particles' constituent de Broglie waves into a series of discrete momentum states. In the δ-kicked accelerator, the linear potential modifies the chaotic classical dynamics only slightly, yet can radically change the quantum behavior. The phases accumulated between consecutive kicks by the momentum states are altered, leading to the creation of quantum accelerator modes (QAM) [7–9]. We realize quantum δ-kicked accelerator dynamics in laser-cooled cesium atoms by the application of short pulses of a vertical standing wave of off-resonant laser light, which constitutes a sinusoidal potential; gravity provides the linear potential. QAM are characterized by a linear (with kick number) momentum transfer to a substantial fraction ($\sim 20\%$) of the atoms. If coherent, this efficient momentum transfer promises applications in atom interferometry [11]. We use a Ramsey-type interference experiment [12] to show that QAM do preserve coherence. We then relate the Ramsey fringe contrast to the fidelity f [13]; by a numerical analysis, we link the behavior of f to the phase space structure generated by a pseudoclassical map recently proposed by Fishman, Guarneri, and Rebuzzini (FGR) [14]. This map is applicable when the interkick evolution time is close to resonant values [15]. Finally, we explain differences in the observed fringe visibilities by examining the effect of the experimental range of kicking strengths.

In our interference experiment the atoms undergo δ-kicked accelerator dynamics, between the application of two $\pi/2$ microwave pulses that couple two atomic hyperfine levels. In the absence of coherence-destroying spontaneous emission, the contrast of any interference fringes is related to the overlap of two initially identical motional states evolved under slightly different chaotic Hamiltonians [16], i.e., the fidelity. It can therefore yield information on the sensitivity of the atoms' evolution to variations in the kicking strength. Strong sensitivity can be considered a quantum signature of chaos, particularly in the semiclassical limit ($\hbar \to 0$), as the eigenstates are sensitive to such variations. Hence the use by Peres [17] of f as a measure of quantum stability.

After magneto-optic trapping and molasses cooling to 5 μK, we prepare around 10^6 freely falling cesium atoms in the $F = 3$, $m_F = 0$ hyperfine level (denoted $|a\rangle$) of the $6^2S_{1/2}$ ground state [18]. The first $\pi/2$ microwave pulse creates an equal superposition of the atoms' internal states, i.e., $|a\rangle \to (|a\rangle - ie^{i\theta}|b\rangle)/\sqrt{2}$, where $|b\rangle$ denotes the $F = 4$, $m_F = 0$ level. The phase θ of this pulse can be changed with respect to that of the second $\pi/2$ pulse, applied following 20 equally spaced 500 ns pulses from a standing wave of light. This is formed by retroreflection of a Ti:sapphire laser beam; its maximum intensity is $\sim 1 \times 10^4$ mW/cm^2 [9], and the light is red detuned by 45 and 35 GHz from the D1 transition for atoms in states $|a\rangle$ and $|b\rangle$, respectively. After the second $\pi/2$ microwave pulse, we measure the momentum distribution in state $|b\rangle$ by a time-of-flight method. For more details of our experimental setup, see Refs. [8,9]. Measurement of a periodic variation with θ in the QAM population in state $|b\rangle$, i.e., interference, directly implies coherent evolution.

In the limit of large detuning, the Hamiltonian is

$$\hat{H} = \hat{H}_a|a\rangle\langle a| + \hat{H}_b|b\rangle\langle b| + \frac{\hbar\omega_{ab}}{2}(|b\rangle\langle b| - |a\rangle\langle a|), \quad (1)$$

where $\hbar\omega_{ab}$ is the energy gap between $|a\rangle$ and $|b\rangle$, and

 0031-9007/03/90(5)/054101(4)$20.00

$$\hat{H}_\sigma = \frac{\hat{p}^2}{2m} + mg\hat{z} - \frac{\hbar\Omega^2 t_p}{8\delta_L^\sigma}[1 + \cos(G\hat{z})]\sum_n \delta(t - nT)$$

is the quantum δ-kicked accelerator Hamiltonian, acting on atoms in internal state $|\sigma\rangle \in \{|a\rangle, |b\rangle\}$. Here $\hat{z}$ is the vertical position, $\hat{p}$ the z momentum, m the particle mass, g the gravitational acceleration, t the time, T the pulsing period, Ω the Rabi frequency, t_p the pulse duration, δ_L^σ the detuning from the D1 transition for the state $|\sigma\rangle$, and $G = 4\pi/\lambda$, where $\lambda = 894$ nm is the laser wavelength, and $\hbar G$ is a grating recoil (the momentum separation of adjacent diffracted states). We denote the amplitude of the phase modulation to atoms in state $|b\rangle$ that results from application of the standing wave as $\phi_d = \Omega^2 t_p/8\delta_L^b$. The experimental mean value of ϕ_d is 0.8π, and, due to the different detuning, that of the corresponding quantity for atoms in state $|a\rangle$ is $\phi_d^a = \phi_d \delta_L^b/\delta_L^a = 0.6\pi$. We thus have effectively two different Hamiltonians, applied to the same initial motional state. The pulse train leads to the creation of a QAM, the momentum of which is the same for the two internal states [8]. We consider pulse periods $T = 60.5$ μs and 74.5 μs, close to $T_{1/2} = 2\pi m/\hbar G^2 = 66.7$ μs, which corresponds to the lowest second-order quantum resonance in the δ-kicked rotor [9,15]. Well-populated QAM involving substantial momentum transfer are then created [7–9].

Figure 1(a) shows the measured final momentum distributions of $|b\rangle$ atoms, for $T = 60.5$ μs. We see a period-2π variation with θ in the QAM population (at around $-17\hbar G$), the visibility V of which is $(21 \pm 2)\%$ [19]. We observe similar fringes for a range of detunings ($\delta_L^b = 20$–40 GHz) and total number of kicks $N = 10$–30, over which V can vary between 10% and 40%. This periodic variation of the population demonstrates interference, and hence that the QAM transfers momentum coherently. At $T = 74.5$ μs [Fig. 1(b)], however, fringes in the QAM (at around $20\hbar G$) are practically invisible, despite the expected coherent nature of the momentum transfer. In Figs. 1(c) and 1(d) numerical simulations [7–9], incorporating the experimental range of ϕ_d (0.3π to 1.2π), also show this difference in the fringe visibility for the two values of T. The range of ϕ_d is due to the Gaussian profile of the standing wave intensity (FWHM ~1 mm) and the spatial extent of the atomic cloud (Gaussian density distribution, FWHM ~1 mm) [9]. As we optimized the overlap of the laser beams with the atomic cloud, the intensity and density maxima can be assumed to be coincident. The calculated visibility is 25% for $T = 60.5$ μs [Fig. 1(c)] but only 8% for $T = 74.5$ μs [Fig. 1(d)].

In order to explain these surprising observations, we introduce the Floquet operator $\hat{F}_b(\phi_d)$. This describes the effect of one kick and the subsequent free evolution on the motional state of atoms in state $|b\rangle$:

$$\hat{F}_b(\phi_d) = \exp(-i[\gamma\hat{\chi} + \hat{\rho}^2/2]/\bar{k})\exp(i\phi_d[1 + \cos\hat{\chi}]). \tag{2}$$

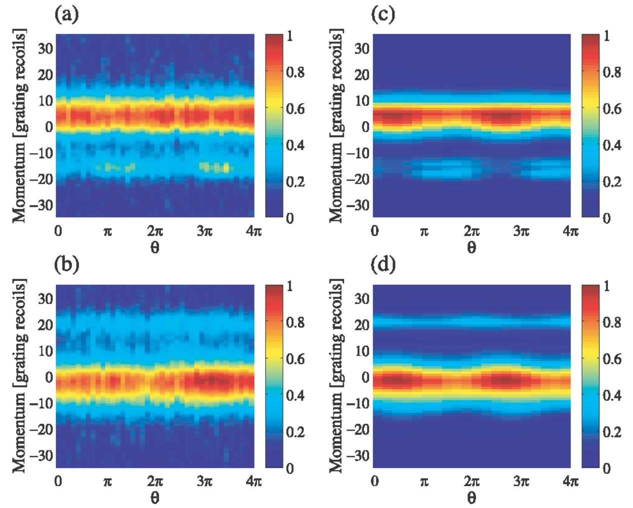

FIG. 1 (color online). Experimental momentum distributions as the microwave phase difference θ is varied in a $\pi/2$—20 kick—$\pi/2$ sequence where $\delta_L^b \sim 35$ GHz, with (a) $T = 60.5$ μs (QAM at $-17\hbar G$), and (b) $T = 74.5\mu$s (QAM at $20\hbar G$). Corresponding numerical momentum distributions, where $\delta_L^b = 35$ GHz, are in (c) and (d). Population arbitrarily normalized to maximum value = 1.

We define $\hat{F}_a(\phi_d)$ analogously for state $|a\rangle$, with ϕ_d replaced by ϕ_d^a [20]. We use scaled position and momentum variables $\chi = Gz$ and $\rho = GTp/m$, while $\gamma = gGT^2$ incorporates gravity, and $\bar{k} = \hbar G^2 T/m = -i[\hat{\chi}, \hat{\rho}]$ is an effective Planck constant [9]. After N pulses an initial plane wave $|q\rangle$ of wave number q evolves to $\hat{F}_\sigma(\phi_d)^N|q\rangle = e^{i\phi N}|\psi_\sigma^q(\phi_d)\rangle$, where $\phi = \phi_d$ or ϕ_d^a. Regarding the initial motional state as an incoherent superposition of $|q\rangle$, the momentum distribution in $|b\rangle$ for a given ϕ_d after the $\pi/2$—N kick—$\pi/2$ sequence, is

$$P_b(\phi_d, p) = \frac{1}{4}\int dqC(q)[|\psi_a^q(\phi_d, p)|^2 + |\psi_b^q(\phi_d, p)|^2] + \frac{1}{2}\left|\int dqC(q)\psi_a^q(\phi_d, p)^*\psi_b^q(\phi_d, p)\right| \times \cos[\phi_I(\phi_d, p) + N\delta\phi_d + \theta], \tag{3}$$

where $\delta\phi_d = \phi_d - \phi_d^a$, $\psi_\sigma^q(\phi_d, p) = \langle p|\psi_\sigma^q(\phi_d)\rangle$, and ϕ_I is the phase of the interference term, i.e., $\int dqC(q)\psi_a^{q*}\psi_b^q = |\int dqC(q)\psi_a^{q*}\psi_b^q|e^{i\phi_I}$, and $C(q)$ describes the initial Gaussian momentum distribution (FWHM = 6 $\hbar G$). The third (interference) term in Eq. (4) is responsible for the appearance of fringes in the accelerated $|b\rangle$ population. We denote the amplitude of the modulation in P_b by $A(\phi_d, p)/2 = |\int dqC(q)\psi_a^q(\phi_d, p)^*\psi_b^q(\phi_d, p)|/2$, where $\int dpA(\phi_d, p)^2 = f(\phi_d)$ is the fidelity for a given ϕ_d.

We have calculated the individual terms of P_b numerically for a wide range of ϕ_d, obtaining as a consequence an important result linking the pseudoclassical analysis of FGR [14] with the quantum stability measure of Peres [17]. Comparison of Figs. 2(a) and 2(c) with Fig. 1 shows that the region in momentum space corresponding to a

QAM is also a region of high A. This remains high up to large values of ϕ_d, continuing beyond the point at which it has decayed to nearly zero in other regions of momentum space. As $f = \int dpA^2$, its large value when determined by integrating over the momenta populated by atoms in the QAM implies that these atoms inhabit a stable region of quantum state space. Small A need not imply low population, as we see in Figs. 2(b) and 2(d). Contrasting Fig. 2(a) with Fig. 2(c), we see that this large value of A extends over a significantly wider range of ϕ_d for $T = 60.5$ μs than for $T = 74.5$ μs. Hence, we can interpret the QAM at $T = 60.5$ μs as being more robust to variations in ϕ_d, i.e., more *stable*, compared with that at $T = 74.5$ μs. However, given our experimental range of ϕ_d, this does not explain the difference in fringe visibilities seen in Fig. 1.

The appearance of QAM in the δ-kicked accelerator is explained in the analysis of FGR [14] by islands of stability in the phase space generated by the map [21]:

$$\tilde{\rho}_{n+1} = \tilde{\rho}_n - \tilde{k}\sin(\chi_n) - \mathrm{sign}(\epsilon)\gamma, \tag{4}$$

$$\chi_{n+1} = \chi_n + \mathrm{sign}(\epsilon)\tilde{\rho}_{n+1}, \tag{5}$$

where the population of a mode is proportional to the size of the corresponding island. This is a *pseudoclassical* $[\epsilon = (\not{k} - 2\pi) \rightarrow 0]$ rather than *semiclassical* $(\not{k} \rightarrow 0)$ limit of the quantum dynamics characterized by the Floquet operator of Eq. (2). We have introduced $\tilde{\rho} = \rho\epsilon/\not{k}$ (in an accelerating frame [14]) and $\tilde{k} = \phi_d|\epsilon|$. Classically, the system is globally chaotic for our parameter regime. Figure 3 shows the pseudoclassical phase spaces generated by iteration of Eqs. (4) and (5) for the experimentally investigated values of $\epsilon = 2\pi(T/T_{1/2} - 1)$, and a range of ϕ_d. When $\phi_d = 0.3\pi$ [Figs. 3(a) and 3(d)], the island is substantially smaller for $T = 74.5$ μs than for $T = 60.5$ μs. For the average experimental value of $\phi_d = 0.8\pi$ [Figs. 3(b) and 3(e)], the islands have both grown to be about the same size. For $\phi_d = 1.5\pi$ [Figs. 3(c) and 3(f)], the island has shrunk dramatically in the case of $T = 74.5$ μs, while at $T = 60.5$ μs the island has not shrunk to the same extent. We therefore conclude that the stable island representing the QAM is much more robust to perturbations in the kicking strength for $T = 60.5$ μs than for $T = 74.5$ μs. The fact that A (and therefore f) remains large at the QAM momentum for a significantly broader range of ϕ_d when $T = 60.5$ μs than for when $T = 74.5$ μs, as shown in Fig. 2, matches the observed greater stability of the island in the pseudoclassical phase space for $T = 60.5$ μs. This is consistent with Peres's identification of the behavior of the fidelity as reflecting stability properties of the phase space in the semiclassical limit [17], even though our experiment is in a pseudoclassical regime, far from semiclassical.

The position of the islands in pseudoclassical phase space in Fig. 3 indicates the region of the QAM's spatial localization. For $T = 60.5$ μs this is where there is zero laser intensity, whereas when $T = 74.5$ μs it is where the

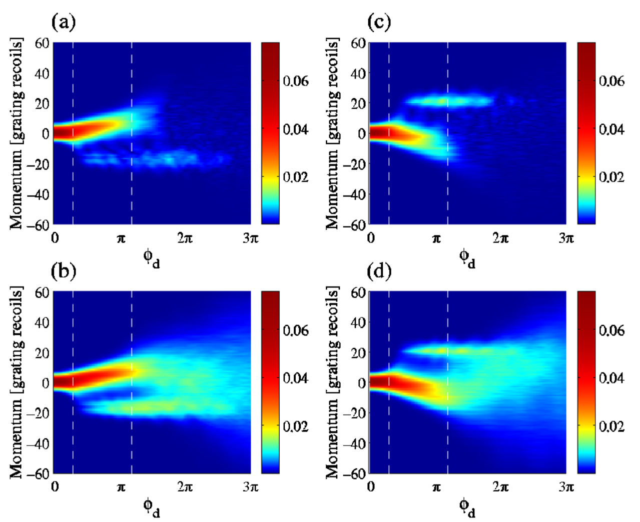

FIG. 2 (color online). Numerical plots of $A/2$ against ϕ_d with $N = 20$, for (a) $T = 60.5$ μs and (c) $T = 74.5$ μs. Plots of the noninterfering population $\int dqC(q)(|\psi_a^q|^2 + |\psi_b^q|^2)/4$ for (b) $T = 60.5$ μs and (d) $T = 74.5$ μs. Dashes demarcate the experimental range of ϕ_d.

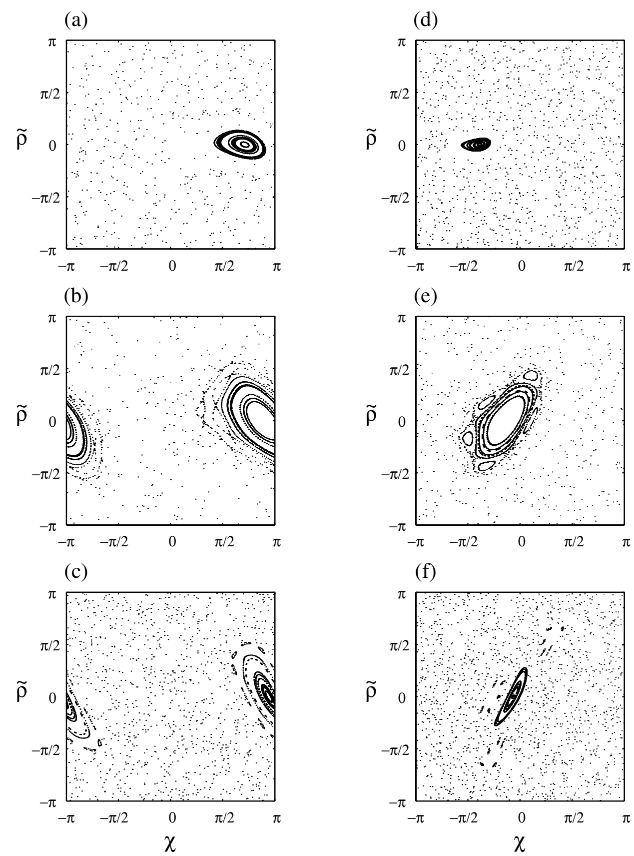

FIG. 3. Stroboscopic Poincaré sections determined by Eqs. (4) and (5) for $T = 60.5$ μs ($\Rightarrow \epsilon = -0.58$), and for (a) $\phi_d = 0.35\pi$, (b) the average experimental value 0.8π, and (c) 1.5π. (d), (e), and (f) show corresponding plots for $T = 74.5$ μs ($\Rightarrow \epsilon = 0.73$). Units are dimensionless.

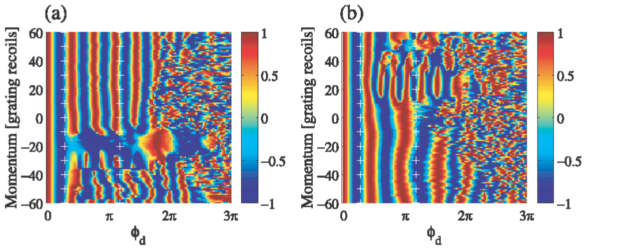

FIG. 4 (color online). Numerical plots of $\cos(\phi_I + N\delta\phi_d)$ against ϕ_d ($N = 20$) for (a) $T = 60.5\ \mu$s and (b) $T = 74.5\ \mu$s. Crosses demarcate the experimental range of ϕ_d.

intensity, and hence phase shift, are maximal. As the phase of the P_b interference term in Eq. (4) depends on the absolute difference between the potentials experienced by $|a\rangle$ and $|b\rangle$, we expect it to depend strongly on ϕ_d for the momenta at which QAM are found when $T = 74.5\ \mu$s, but not when $T = 60.5\ \mu$s. This is confirmed by Figs. 4(a) and 4(b) where $\cos(\phi_I + N\delta\phi_d + \theta)$ is plotted as a function of p and ϕ_d for constant θ (set to 0 for convenience) for $T = 60.5\ \mu$s and $T = 74.5\ \mu$s. At the QAM momentum, the value of $\cos(\phi_I + N\delta\phi_d)$ at $T = 60.5\ \mu$s is almost independent of ϕ_d, whereas at $T = 74.5\ \mu$s there is an approximate frequency doubling, relative to other momenta. This effect explains the presence or absence of interference fringes in Fig. 1. For a single value of ϕ_d the visibility of the fringes at both $T = 60.5\ \mu$s and $T = 74.5\ \mu$s is high, but Figs. 4(a) and 4(b) show that integration over the experimental range of ϕ_d causes a greater reduction in visibility at $T = 74.5\ \mu$s than at $T = 60.5\ \mu$s. At larger ϕ_d than in our experiment, there is a breakdown of structure in plots of $\cos(\phi_I + N\delta\phi_d)$, coinciding with a falloff in A [see Figs. 2(a) and 2(c)]. As ϕ_I is determined numerically from complex interference terms, however, one should be careful about attaching significance to values of $\cos(\phi_I + N\delta\phi_d)$ where A is close to zero.

In summary, we have performed a Ramsey-type interference experiment and thus demonstrated the coherence of the production of quantum accelerator modes, and hence their suitability for applications in atom interferometry. Numerically, we have found the accelerator modes to correspond to regions of greater quantum stability, as quantified by the fidelity. This is consistent with the presence of stable regions in the phase space of a pseudoclassical limit of δ-kicked accelerator dynamics, rather than the globally chaotic behavior of the semiclassical limit. These regions dictate the position of the accelerator modes' spatial localization, allowing us to explain the lack of fringes for the accelerator mode at certain pulse periods, due to the experimental range of kicking strengths. Our investigation of coherence in quantum accelerator modes has allowed observation of their quantum-stable dynamics in this classically chaotic system.

We thank R. Bach, K. Burnett, S. Fishman, I. Guarneri, L. Rebuzzini, and S. Wimberger for stimulating discussions. We acknowledge support from the UK EPSRC, the Paul Instrument Fund of The Royal Society, and the EU through the TMR "Cold Quantum Gases" network.

[1] W. H. Zurek, Phys. Today **44**, No. 10, 36 (1991).
[2] F. Haake, *Quantum Signatures of Chaos* (Springer-Verlag, Berlin, 2001), 2nd ed.
[3] J. E. Bayfield *et al.*, Phys. Rev. Lett. **63**, 364 (1989); M. Arndt *et al.*, *ibid.* **67**, 2435 (1991); P. M. Koch and K. A. H. van Leeuwen, Phys. Rep. **255**, 289 (1995).
[4] S. Sridhar and E. J. Heller, Phys. Rev. A **46**, R1728 (1992); A. Kudrolli *et al.*, Phys. Rev. E **49**, R11 (1994).
[5] P. B. Wilkinson *et al.*, Nature (London) **380**, 608 (1996); J. P. Bird *et al.*, Phys. Rev. Lett. **82**, 4691 (1999); P. B. Wilkinson *et al.*, *ibid.* **86**, 5466 (2001).
[6] F. L. Moore *et al.*, Phys. Rev. Lett. **75**, 4598 (1995); B. G. Klappauf *et al.*, *ibid.* **81**, 1203 (1998); H. Ammann *et al.*, *ibid.* **80**, 4111 (1998); W. K. Hensinger *et al.*, Nature (London) **412**, 52 (2001); D. A. Steck *et al.*, Science **293**, 274 (2001).
[7] M. K. Oberthaler *et al.*, Phys. Rev. Lett. **83**, 4447 (1999).
[8] R. M. Godun *et al.*, Phys. Rev. A **62**, 013411 (2000).
[9] M. B. d'Arcy *et al.*, Phys. Rev. E **64**, 056233 (2001).
[10] G. Casati *et al.*, in *Stochastic Behavior in Classical and Quantum Hamiltonian Systems* (Springer-Verlag, New York, 1979).
[11] P. Berman, *Atom Interferometry* (Academic Press, San Diego, 1997).
[12] *Molecular Beams*, edited by N. F. Ramsey (Oxford University Press, Oxford, 1986).
[13] N. R. Cerruti and S. Tomsovic, Phys. Rev. Lett. **88**, 054103 (2002); Y. S. Weinstein *et al.*, *ibid.* **89**, 214101 (2002); G. Benenti and G. Casati, Phys. Rev. E **65**, 066205 (2002).
[14] S. Fishman, I. Guarneri, and L. Rebuzzini, Phys. Rev. Lett. **89**, 084101 (2002); nlin.CD/0202047.
[15] W. H. Oskay *et al.*, Opt. Commun. **179**, 137 (2000); M. B. d'Arcy *et al.*, Phys. Rev. Lett. **87**, 074102 (2001).
[16] S. A. Gardiner *et al.*, Phys. Rev. Lett. **79**, 4790 (1997).
[17] A. Peres, *Quantum Theory: Concepts and Methods* (Kluwer Academic Publishers, Dordrecht, 1993); R. Schack and C. M. Caves, Phys. Rev. E **53**, 3257 (1996); **53**, 3387 (1996); G. Garcia de Polavieja, Phys. Rev. A, **57**, 3184 (1998).
[18] Here F is the total angular momentum, and m_F is the projection on the quantization axis.
[19] We define the visibility by $V = (S_{\max} - S_{\min})/(S_{\max} + S_{\min})$, where S is the QAM population in $|b\rangle$.
[20] As ϕ_d^a is determined by ϕ_d, $\hat{F}_a$ is a function of ϕ_d.
[21] Here χ_n and $\tilde{\rho}_n$ specify χ and $\tilde{\rho}$ just prior to kick $n + 1$, as in Ref. [9], rather than just after kick n, as in Ref. [14].